SIAM J. SCI. COMPUT.
Vol. 25, No. 6, pp. 2004–2028


# NUMERICAL SIMULATION OF THE SMOLUCHOWSKI COAGULATION EQUATION*

FRANCIS FILBET† AND PHILIPPE LAURENÇOT‡

**Abstract.** In this paper, we develop a numerical scheme for the Smoluchowski coagulation equation, which relies on a conservative formulation and a finite volume approach. Several numerical simulations are performed to test the validity of the scheme and the expected behavior of the model. In particular the gelation phenomenon and the long time behavior of the solution are numerically studied.

**Key words.** Smoluchowski coagulation equation, self-similar variables, finite volume method

**AMS subject classifications.** 65R20, 82C05

**DOI.** 10.1137/S1064827503429132

**1. Introduction.** The Smoluchowski coagulation equation is a mean-field model for the growth of clusters (particles, droplets, etc.) by binary coalescence; that is, the driving growth mechanism is the merger of two particles into a single one. In the simple situation where each particle is fully identified by its volume, it describes the dynamics of the volume distribution function, $f = f(t,x) \ge 0$, of particles of volume $x > 0$ at time $t \ge 0$ and reads [12, 38]

$$\partial_t f = Q_c(f)\,, \quad (t,x) \in \mathbb{R}_+^2\,, \tag{1}$$

$$f(0) = f_0\,, \quad x \in \mathbb{R}_+\,, \tag{2}$$

where $\mathbb{R}_+ := (0,+\infty)$ and the coagulation reaction term $Q_c(f)$ is given by

$$Q_c(f)(x) = \frac{1}{2}\int_0^x a(x',x-x')\ f(x')\ f(x-x')\ dx' - \int_0^\infty a(x,x')\ f(x)\ f(x')\ dx' \tag{3}$$

for $x \in \mathbb{R}_+$. The first integral in $Q_c(f)$ accounts for the formation of particles with volume, $x$ resulting from the merger of two particles with respective volumes $x'$ and $x - x'$, $x' \in (0,x)$. The second integral in $Q_c(f)$ describes the loss of particles with volume $x$ by coagulation with other particles. The coagulation coefficient, $a = a(x,x')$, characterizes the rate at which the coalescence of two particles with respective volumes $x$ and $x'$ produces a particle of volume $x+x'$ and is a nonnegative symmetric function,

$$0 \le a(x,x') = a(x',x)\,, \quad (x,x') \in \mathbb{R}_+^2\,.$$

At this point, observe that, during each coagulation event, the total volume of particles is conserved while the number of particles decreases. In terms of $f$, the total number

*Received by the editors June 3, 2003; accepted for publication (in revised form) September 29, 2003; published electronically May 25, 2004. This research was partially supported by the ACI "Jeunes Chercheurs" *Analyse mathématique et simulation numérique de particules chargées*, n° 2000 − 2526 and by the EU network HYKE, contract number HPRN-CT-2002-00282.
http://www.siam.org/journals/sisc/25-6/42913.html

†Mathématiques et Applications, Physique Mathématique d'Orléans, CNRS UMR 6628, Université d'Orléans, B.P. 6759, F–45067 Orléans cedex 2, France (filbet@labomath.univ-orleans.fr).

‡Mathématiques pour l'Industrie et la Physique, CNRS UMR 5640, Université Paul Sabatier – Toulouse 3, 118 route de Narbonne, F–31062 Toulouse cedex 4, France (laurenco@mip.ups-tlse.fr).

of particles $M_0(t)$ and the total volume of particles $M_1(t)$ at time $t \ge 0$ are given by

$$M_0(t) := \int_0^\infty f(t,x)\ dx\,, \quad M_1(t) := \int_0^\infty x\ f(t,x)\ dx\,. \tag{4}$$

While it is straightforward to check that $M_0$ is a nonincreasing function of time, it is well known that $M_1$ might not remain constant throughout time evolution for some coagulation coefficient $a$ [17, 33]. More precisely, if $a$ increases sufficiently rapidly for large $x$, $x'$, the larger the particles are, the faster they merge. A runaway growth then takes place, producing particles with "infinite" volume in finite time which are removed from the system. Consequently, $M_1$ starts to decrease, a phenomenon usually called the occurrence of gelation.

The purpose of this work is to present and study a numerical scheme for the coagulation equation (1) and to investigate numerically the occurrence of gelation, when it takes place, and the large time behavior otherwise. Numerical methods have already been developed to solve (1) or its discrete counterpart; see, e.g., [16, 26, 30] for deterministic methods, [2, 8, 14, 15, 22, 37] for stochastic methods, and the references therein. However, it seems that none of the above-mentioned deterministic numerical approaches make use of an alternative formulation of the coagulation equation (1) in a "conservative" form which has been used in [35, 40] for different purposes. More precisely, it has been pointed out in [35, 40] that the coagulation equation (1) may also be written as follows:

$$x\ \partial_t f = -\partial_x J(f)\,, \quad (t,x) \in \mathbb{R}_+^2\,, \tag{5}$$

where

$$J(f)(x) := \int_0^x \int_{x-u}^\infty u\ a(u,v)\ f(u)\ f(v)\ dvdu\,, \quad x \in \mathbb{R}_+\,. \tag{6}$$

We then take advantage of the formulation (5) and propose a numerical scheme to solve the coagulation equation in the spirit of finite volume methods. Before describing the scheme more precisely, let us emphasize here that the formulation (5) does not imply that $M_1$ stays constant throughout time evolution in contrast to what a direct integration of (5) over $\mathbb{R}_+$ would indicate. The key observation is that the integrability properties of $f$ vary with time and do not guarantee that $J(f)(t,x) \to 0$ as $x \to +\infty$ for every time $t \ge 0$. The occurrence of the gelation phenomenon actually coincides with a nonvanishing limit of $J(f)(t,x) \to 0$ as $x \to +\infty$ for some time $t$. Indeed, observe that it follows from (5) that

$$\lim_{X \to +\infty} \int_0^t J(f)(s,X)\ ds = M_1(0) - M_1(t) \quad \text{for} \quad t > 0\,.$$

In the next section, we describe the discretization of (5), a preliminary step being to suitably truncate the second integral in (6). We next compare the numerical solutions with exact ones available in the literature. After this validation step, we perform several numerical computations to study the gelation phenomenon and the large time behavior. In section 3, we focus on the gelation phenomenon and observe the expected loss of matter in finite time in the simulations and the simultaneous blow-up of higher moments of $f$ as well. The last section is devoted to the study of the long time behavior of $f$, when the total volume remains constant through time evolution. Since the support of $f$ becomes larger and larger, the numerical simulations

for large times are very sensitive to the value of the truncation parameter. To remedy this drawback, we use a natural rescaling with respect to volume and time and a well-suited nonuniform mesh. The latter is needed because the distribution function develops a polynomial singularity for small volumes in large times.

**2. The numerical method.** Since the volume variable $x$ ranges in the unbounded interval $\mathbb{R}_+$, the first step is to reduce the computation to a finite interval. One possibility is to perform a change of variables which maps $\mathbb{R}_+$ onto $(0,1)$ (such as $x \mapsto 1/(1+x)$), and this approach has been used in [16]. However, it seems more difficult to control the distribution of mesh points. The most widely used approach is to truncate the volume variable to some maximal value $R$. In that case, one has to choose a suitable truncation $J^R(f)$ of the coagulation term $J(f)$ among several possibilities. This issue is discussed in [3, 6], and we will only consider two of these possibilities below. The conservative one is

$$J_c^R(f)(x) := \int_0^x \int_{x-u}^{R-u} u\ a(u,v)\ f(u)\ f(v)\ dvdu\,, \quad x \in (0,R)\,. \tag{7}$$

In that case, we have $J_c^R(f)(R) = J_c^R(f)(0) = 0$ so that the solution $f_R$ to

$$x\ \partial_t f_R = -\partial_x J_c^R(f_R)\,, \quad (t,x) \in \mathbb{R}_+ \times (0,R)\,, \tag{8}$$

satisfies the total volume conservation

$$\int_0^R x\ f_R(t,x)\ dx = \int_0^R x\ f_R(0,x)\ dx\,, \quad t \in \mathbb{R}_+\,.$$

The second truncation is the nonconservative one,

$$J_{nc}^R(f)(x) := \int_0^x \int_{x-u}^{R} u\ a(u,v)\ f(u)\ f(v)\ dvdu\,, \quad x \in (0,R)\,, \tag{9}$$

which was first considered in [3]. In that case, $J_{nc}^R(f)(R) \ge 0$ so that the total volume of the solution $f_R$ to

$$x\ \partial_t f_R = -\partial_x J_{nc}^R(f_R)\,, \quad (t,x) \in \mathbb{R}_+ \times (0,R)\,, \tag{10}$$

is nonincreasing with respect to time. This last approximation is particularly well suited for reproducing the gelation phenomenon [3, 6]. Such a truncation is used in [26] to perform numerical simulations on the original formulation (1) of the coagulation equation.

When $a(x,x')/(x\ x') \to 0$ as $x + x' \to +\infty$, convergence as $R \to +\infty$ of the solutions to (8) toward a solution of (5) has been shown in [13, 39]. Under the same assumption, a similar result can be proved for solutions to (10) by using the approach developed in [28]. In both cases, the main purpose of the above-mentioned papers is to establish existence results for (5). Two additional facts are worth pointing out here: first, the previous growth assumption on $a(x,x')$ does not exclude coagulation coefficients for which the occurrence of gelation takes place (such as $a(x,x') = (x\ x')^\alpha$ for $1/2 < \alpha \le 1$). Second, when gelation does not take place, it can be shown that the solutions to (8) and (10) both converge toward a solution to (5) satisfying $M_1(t) = M_1(0)$ for $t \ge 0$ (see [13, 18] for the conservative case and [20] for the nonconservative case). Next, only the convergence for the nonconservative approximation (9), (10) is valid when $a(x,x') \sim x\ x'$ for large $x, x'$ [27]. Since the conservative approximation (7) is not suitable to study the gelation phenomenon, we will only consider the nonconservative one in what follows.

**2.1. The numerical scheme.** Having reduced the computation to a bounded interval, the second step is to introduce the time and volume discretizations. To this end, let $h \in (0,1)$, let $I^h$ be a large integer, and denote by $(x_{i-1/2})_{i\in\{0,\dots,I^h\}}$ a mesh of $(0,R)$, where

$$x_{-1/2} = 0\,, \quad x_i = (x_{i-1/2} + x_{i+1/2})/2\,, \quad \Delta x_i = x_{i+1/2} - x_{i-1/2} \le h\,, \tag{11}$$

and $\Lambda_i^h = [x_{i-1/2}, x_{i+1/2})$ for $i \ge 0$. Owing to the formulation (5), it seems natural to compute $g(t,x) = x\, f(t,x)$ rather than $f(t,x)$. We then define the approximation $g^{0,h}$ of the initial datum $g_0(x) = x\, f_0(x)$ by

$$g_i^{0,h} = \frac{1}{\Delta x_i} \int_{\Lambda_i^h} g_0(x)\, dx\,. \tag{12}$$

Denoting by $g_i^n$ an approximation of the mean value of $g(t^n,x) = x\, f(t^n,x)$ on $\Lambda_i^h$ for $i \in \{0,\dots,I^h\}$ and $t^n = n\,\Delta t$, the numerical scheme to be studied in this paper reads

$$g_i^{n+1} = g_i^n - \frac{\Delta t}{\Delta x_i}\left(J_{i+1/2}^{h,n} - J_{i-1/2}^{h,n}\right)\,, \quad 0 \le i \le I^h\,, \tag{13}$$

for $n \in \{0,\dots,N-1\}$, with the initial datum $(g_i^{0,h})_{0\le i\le I^h}$ defined in (12), where $J_{i+1/2}^{h,n}$ is given by

$$J_{i+1/2}^{h,n} = \sum_{k=0}^{i} \Delta x_k g_k^n \left\{ \sum_{j=\alpha_{i,k}}^{I^h} \int_{\Lambda_j^h} \frac{a(x',x_k)}{x'}\, dx'\, g_j^n + \int_{x_{i+1/2}-x_k}^{x_{\alpha_{i,k}-1/2}} \frac{a(x',x_k)}{x'}\, dx'\, g_{\alpha_{i,k}-1}^n \right\} \tag{14}$$

and the integer $\alpha_{i,k}$ corresponds to the index of the cell such that $x_{i+1/2} - x_k \in \Lambda_{\alpha_{i,k}-1}^h$. Notice that the approximate flux $J_{i+1/2}^{h,n}$ is an approximation for $-1 \le i \le I^h$ of

$$\begin{aligned} J_{nc}^R(f)(x_{i+1/2}) &= \int_0^{x_{i+1/2}} \int_{x_{i+1/2}-x^*}^R a(x',x^*)\, x^*\, f(x^*)\, f(x')\, dx'\, dx^* \\ &= \sum_{k=0}^{i} \int_{\Lambda_k^h} x^*\, f(x^*) \int_{x_{i+1/2}-x^*}^R a(x',x^*)\, f(x')\, dx'\, dx^*\,. \end{aligned}$$

From the scheme (13), we can define an approximation of $g(t,x) = x\, f(t,x)$ by

$$g^h(t,x) = g_i^n\,, \qquad (t,x) \in [t^n, t^{n+1}) \times \Lambda_i^h\,. \tag{15}$$

Before presenting some numerical experiments, let us first investigate some basic properties of the scheme (13).

PROPOSITION 2.1. *Under the stability condition on the time step,*

$$\Delta t\, \sup_{i,n} \left( \int_{\delta_h}^R \frac{a(x_i,x')}{x'}\, g^h(t^n,x')\, dx' \right) < 1\,, \tag{16}$$

*where $\delta_h = \min\{\Delta x_i/2; i = 0,\dots,I^h\}$, the function $g^h$ is nonnegative and its total volume is a nonincreasing function of time; that is,*

$$\sum_{i=0}^{I^h} \Delta x_i\, g_i^{n+1} \le \sum_{i=0}^{I^h} \Delta x_i\, g_i^n\,, \qquad 0 \le n \le N-1\,. \tag{17}$$

*Moreover, if* $\varphi : [0,+\infty) \to [0,+\infty)$ *is a nonincreasing function, we have*

$$\sum_{i=0}^{I^h} \Delta x_i \ \varphi(x_i) \ g_i^{n+1} \le \sum_{i=0}^{I^h} \Delta x_i \ \varphi(x_i) \ g_i^n \,. \tag{18}$$

*Proof.* For $(i,j) \in \{0,\ldots,I^h\}^2$, we introduce the notation

$$A_{i,j} = \int_{\Lambda_i^h} \frac{a(x',x_j)}{x'} \, dx', \quad B_{i,j} = \int_{x_{i+1/2}-x_j}^{x_{\alpha_{i,j}-1/2}} \frac{a(x',x_j)}{x'} \, dx'. \tag{19}$$

We proceed by induction and first notice that $g^h(0)$ is nonnegative. Assume next that the function $g^h(t^n)$ is nonnegative. We have

$$\begin{aligned}
J_{i+1/2}^{h,n} &= \sum_{k=0}^{i} \Delta x_k g_k^n \left\{ \sum_{j=\alpha_{i,k}}^{I^h} A_{j,k} \, g_j^n + B_{i,k} \, g_{\alpha_{i,k}-1}^n \right\} \\
&= \Delta x_i g_i^n \left\{ \sum_{j=\alpha_{i,i}}^{I^h} A_{j,i} \, g_j^n + B_{i,i} \, g_{\alpha_{i,i}-1}^n \right\} \\
&\quad + \sum_{k=0}^{i-1} \Delta x_k g_k^n \sum_{j=\alpha_{i-1,k}}^{I^h} A_{j,k} \, g_j^n \ - \sum_{k=0}^{i-1} \Delta x_k g_k^n \sum_{j=\alpha_{i-1,k}}^{\alpha_{i,k}-1} A_{j,k} \, g_j^n \\
&\quad + \sum_{k=0}^{i-1} \Delta x_k g_k^n B_{i,k} \, g_{\alpha_{i,k}-1}^n \,.
\end{aligned}$$

If $\alpha_{i,k} = \alpha_{i-1,k}$, we have $B_{i,k} \le B_{i-1,k}$ and

$$\begin{aligned}
J_{i+1/2}^{h,n} &\le \Delta x_i g_i^n \left\{ \sum_{j=\alpha_{i,i}}^{I^h} A_{j,i} \, g_j^n + B_{i,i} \, g_{\alpha_{i,i}-1}^n \right\} \\
&\quad + \sum_{k=0}^{i-1} \Delta x_k g_k^n \sum_{j=\alpha_{i-1,k}}^{I^h} A_{j,k} \, g_j^n \ + \sum_{k=0}^{i-1} \Delta x_k g_k^n B_{i-1,k} \, g_{\alpha_{i,k}-1}^n \\
&\le \Delta x_i g_i^n \left\{ \sum_{j=\alpha_{i,i}}^{I^h} A_{j,i} \, g_j^n + B_{i,i} \, g_{\alpha_{i,i}-1}^n \right\} + J_{i-1/2}^{h,n} \,.
\end{aligned}$$

If $\alpha_{i,k} \neq \alpha_{i-1,k}$, then $\alpha_{i,k} > \alpha_{i-1,k}$ and

$$\begin{aligned}
J_{i+1/2}^{h,n} &\le \Delta x_i g_i^n \left\{ \sum_{j=\alpha_{i,i}}^{I^h} A_{j,i} \, g_j^n + B_{i,i} \, g_{\alpha_{i,i}-1}^n \right\} \\
&\quad + J_{i-1/2}^{h,n} - \sum_{k=0}^{i-1} \Delta x_k g_k^n A_{\alpha_{i,k}-1,k} \, g_{\alpha_{i,k}-1}^n \\
&\quad + \sum_{k=0}^{i-1} \Delta x_k g_k^n B_{i,k} \, g_{\alpha_{i,k}-1}^n \\
&\le \Delta x_i g_i^n \left\{ \sum_{j=\alpha_{i,i}}^{I^h} A_{j,i} \, g_j^n + B_{i,i} \, g_{\alpha_{i,i}-1}^n \right\} + J_{i-1/2}^{h,n} \,,
\end{aligned}$$

since $B_{i,k} \le A_{\alpha_{i,k}-1,k}$. Then, in both cases, it follows from the stability condition (16) that

$$J^{h,n}_{i+1/2} - J^{h,n}_{i-1/2} \le \frac{\Delta x_i}{\Delta t} g^n_i,$$

whence $g^{n+1}_i \ge 0$ by (13).

Next, the time monotonicity (17) of the total volume of $g^h$ follows at once from the nonnegativity of $g^h$ by summing (13) with respect to $i$.

Finally, let $\varphi : [0,+\infty) \to [0,+\infty)$ be a nonincreasing function. It follows from (13) that

$$\varphi(x_i) g^{n+1}_i = \varphi(x_i) g^n_i - \varphi(x_i) \frac{\Delta t}{\Delta x_i} \left( J^{h,n}_{i+1/2} - J^{h,n}_{i-1/2} \right) .$$

Multiplying the above equality by $\Delta x_i$ and summing the resulting identities over $i$, we infer from the positivity of $J^{h,n}_{I^h-1/2}$ that

$$\begin{aligned} \sum_{i=0}^{I^h} \Delta x_i \, \varphi(x_i) g^{n+1}_i &\le \sum_{i=0}^{I^h} \Delta x_i \, \varphi(x_i) g^n_i + \Delta t \sum_{i=1}^{I^h} J^{h,n}_{i-1/2} \left( \varphi(x_i) - \varphi(x_{i-1}) \right) \\ &\le \sum_{i=0}^{I^h} \Delta x_i \, \varphi(x_i) g^n_i \, , \end{aligned}$$

whence (18). □

REMARK 2.2. *If $\varphi \in \mathcal{C}^1([0,+\infty))$ is a nonincreasing and nonnegative function, it readily follows from* (5) *that any solution $f$ to* (5) *is such that*

$$t \longmapsto \int_0^\infty x \, \varphi(x) \, f(t,x) dx \quad \textit{is nonincreasing.}$$

*Inequalities* (17) *and* (18) *are discrete analogues of this property.*

In general, the coefficients $A_{i,j}$ and $B_{i,j}$ given by (19) cannot be explicitly computed, and we use here a simple second order quadrature formula (midpoint formula). In addition, a Runge–Kutta scheme is implemented for the time discretization to guarantee a second order accuracy.

**2.2. Comparison with explicit solutions.** As a first step toward the validation of our scheme, we compare the numerical solutions with the few explicit available solutions to (1).

We first consider the constant kernel $a(x,x') \equiv 1$: in that case, given $M^0_0 > 0$, an explicit solution to (1) is given by

$$f(t,x) = M^2_0(t) \, \exp(-M_0(t) \, x) \quad \text{with} \quad M_0(t) = \frac{2 \, M^0_0}{2 + M^0_0 \, t} \tag{20}$$

for $(t,x) \in \mathbb{R}^2_+$, where $M_0(t)$ is the total number of particles defined by (4). The numerical solution obtained with the scheme (13) is then in good agreement with the exact solution, as shown in Figures 1 and 2. In Figure 1, we report the $L^1$-discrete error norm

$$\epsilon_h(t^n) = \sum_{i=0}^{I^h} \Delta x_i |g^h(t^n) - x_i \, f(t^n, x_i)|, \tag{21}$$

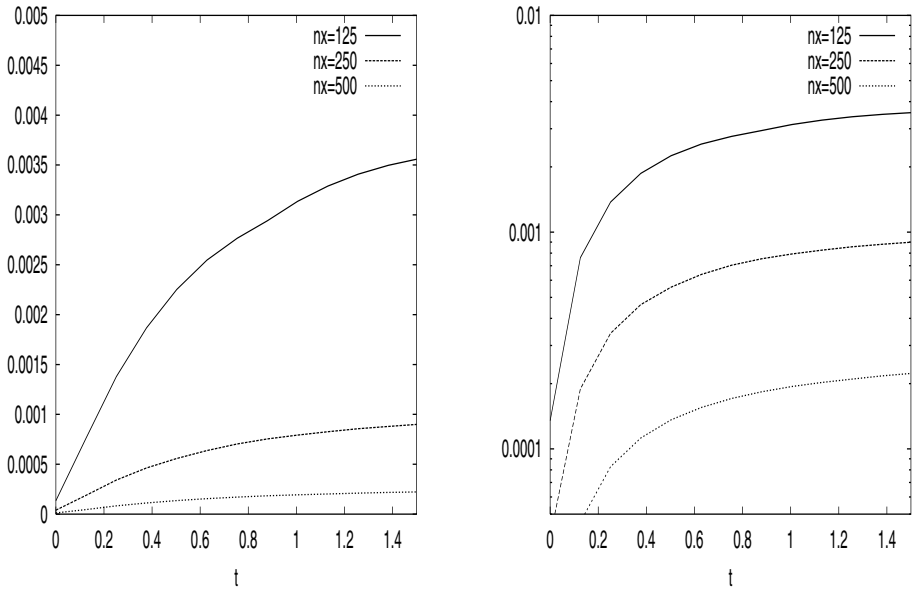


FIG. 1. *Exact solution $a \equiv 1$: Time evolution of the $L^1$-discrete error norm in linear and log scale for $n_x = 125, 250, 500$.*

where $f$ is given by (20). We have computed different approximations using a number of points $n_x = 125$, 250, and 500, whereas the truncation parameter $R$ is fixed to $R = 50$. The scheme is second order accurate as expected, since the numerical error $\epsilon_h$ is proportional to $h^2$.

The second test we perform is for the multiplicative coagulation kernel $a(x, x') = x\,x'$. In that case, the gelation phenomenon is known to occur, and it is also possible to compute an explicit solution [17],

$$f(t,x) = \exp(-T\,x)\,\frac{I_1\left(2\,x\,t^{1/2}\right)}{x^2\,t^{1/2}}\,, \tag{22}$$

corresponding to the initial datum $f(0,x) = \exp(-x)/x$, where

$$T = \begin{cases} 1+t & \text{if } t \le 1\,, \\ 2\,t^{1/2} & \text{otherwise,} \end{cases} \tag{23}$$

and $I_1$ is the modified Bessel function of the first kind

$$I_1(x) = \frac{1}{\pi}\int_0^\pi \exp(x\,\cos\theta)\,\cos\theta\,d\theta.$$

For this solution, the total volume $M_1(t)$ defined by (4) satisfies $M_1(t) = 1$ if $t \in [0,1]$ and $M_1(t) = t^{-1/2}$ if $t \ge 1$ (and the gelation phenomenon takes place at $t = 1$). We are, however, mainly interested in this section in the accuracy of the scheme and postpone a more detailed discussion on the gelation phenomenon to the next section. To keep the second order accuracy, a second order Runge–Kutta scheme is used for the time discretization, whereas the flux $J^{h,n}_{i+1/2}$ is still given by (14). Here again, we observe that the numerical solution agrees with the exact one; see Figures 3

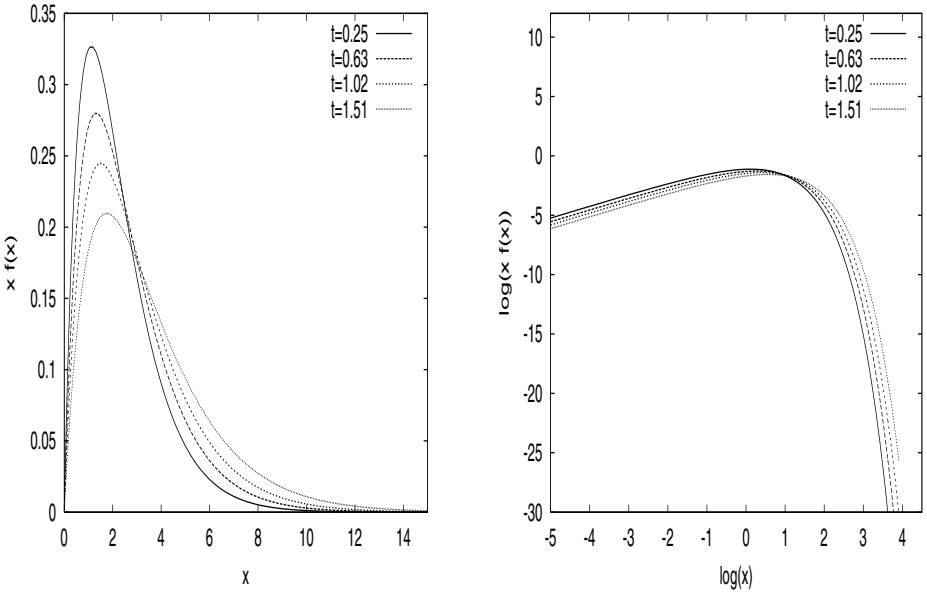


FIG. 2. *Exact solution $a \equiv 1$: Time evolution of the approximated distribution $x\, f(t,x)$ at times $t = 0.25$, 0.63, 1.02, and 1.51 in linear and log scale.*

and 4. In addition, it is clear from Figure 3 that the scheme is second order accurate. Nevertheless, this numerical test is much more difficult than the previous one because of the unboundedness of $a$. Indeed, the support of the distribution function is strongly increasing with respect to time when $a(x, x') = x\, x'$ (see Figures 2 and 4 in log scale). Therefore, a large truncation parameter ($R = 2500$) is needed in order to avoid a loss of matter due to the truncation.

The above two examples already illustrate the importance of the choice of the truncation parameter $R$. Indeed, the effect of coalescence is to "shift" the distribution function $f$ to the right as time goes by. Rapidly increasing coagulation coefficients then induce a faster transfer of matter toward larger and larger volumes, and a larger truncation parameter $R$ has to be chosen accordingly (compare the choice of $R$ in the above two examples). In addition, as we shall see below, a solution with a rapidly decaying initial datum is expected to keep the same decay through time evolution as long as no gelation occurs. Upon the occurrence of gelation, the solution develops an algebraic tail which again requires a large truncation parameter $R$ to obtain accurate results.

**3. Occurrence of gelation.** This section is devoted to a numerical study of the gelation phenomenon, that is, the possible loss of matter during the time evolution. After recalling some basic facts on this phenomenon in section 3.1, we present our numerical results in section 3.2.

**3.1. The gelation phenomenon.** As already mentioned in the introduction, when the coagulation coefficient $a$ increases sufficiently rapidly for large $x, x'$, a runaway growth takes place and leads to the formation of a particle of "infinite volume" in finite time. Since no such particle is taken into account in the Smoluchowski coagulation equation (1), some matter escapes from the system of particles. As a consequence,

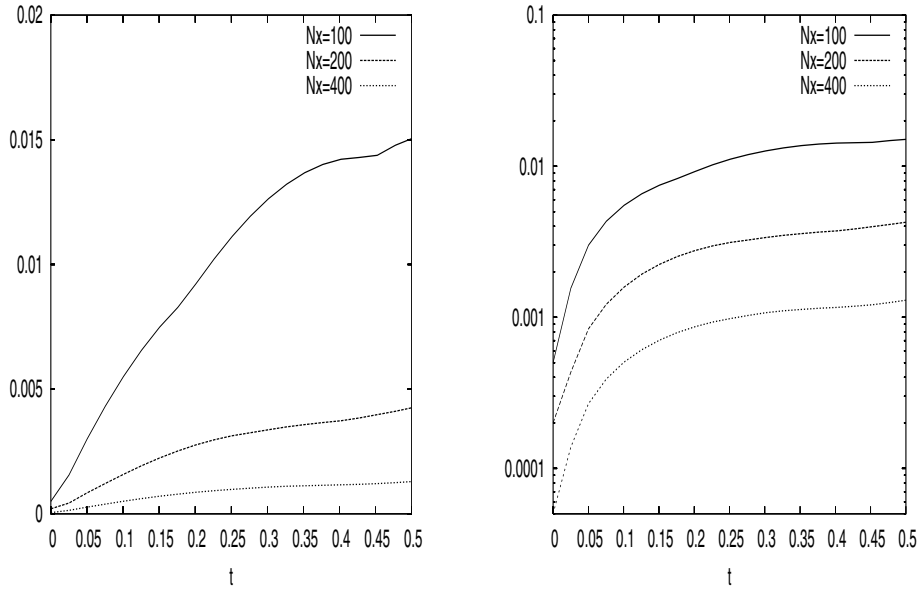


FIG. 3. *Exact solution $a \equiv x\,x'$: Time evolution of the discrete error $L^1$-norm in linear and log scale.*

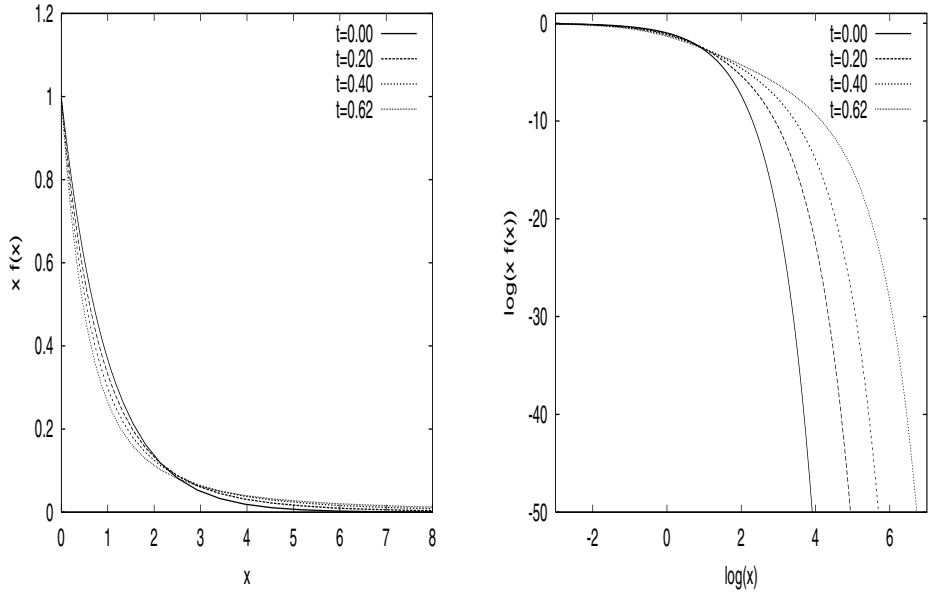


FIG. 4. *Exact solution $a \equiv x\,x'$: Time evolution of $x\,f(t,x)$ at time $t = 0$, 0.2, 0.4, and 0.62 in linear and log scale.*

the total volume $M_1$ defined in (4) decreases with time, and the gelation time $T_{gel}$ is defined by

$$T_{gel} := \inf \left\{ t \ge 0 \,, \quad \int_0^\infty x\ f(t,x)\ dx < \int_0^\infty x\ f(0,x)\ dx \right\} \in [0, +\infty] \,. \tag{24}$$

We then say that gelation occurs if $T_{gel} < +\infty$.

An elementary proof that $T_{gel} < +\infty$ was given in [33] when $a(x, x') = x\, x'$, and a central issue in the physical literature in the eighties was to figure out for which coagulation coefficients $a$ the gelation time $T_{gel}$ is finite. We restrict our discussion here to the model case

$$a(x, x') = x^\mu\ (x')^\nu + x^\nu\ (x')^\mu \,, \qquad 0 \le \mu \le \nu \le 1 \,. \tag{25}$$

It was shown that $T_{gel} < +\infty$ for $\mu = \nu = 1$ [33] and that gelation cannot take place (i.e., $T_{gel} = +\infty$) if $\lambda := \mu + \nu \le 1$ [4, 41]. In the remaining case, $\lambda \in (1, 2)$, particular solutions with a finite gelation time were constructed in [6, 10, 32], which supported the conjecture that $T_{gel} < +\infty$ for every initial data with finite total volume whenever $\lambda \in (1, 2)$ [17, 23, 34]. This conjecture was only recently successfully proven in [24] with a probabilistic approach and in [19] with deterministic arguments. Once gelation is known to occur, a natural question is to determine $T_{gel}$ and to investigate the behavior of $f(t)$ at the gelation time. Formal arguments from the physical literature (see, e.g., [23, 34] and the references therein) indicate that

$$f(T_{gel}, x) \underset{x \to +\infty}{\sim} A\ x^{-(\lambda+3)/2} \,, \tag{26}$$

while the gelation time coincides with the blow-up time of the moment of order $(1 + \lambda)/2$ of $f$, where the moment $M_\ell$ of order $\ell \ge 0$ of $f$ is defined by

$$M_\ell(t) := \int_0^\infty x^\ell\ f(t,x)\ dx \,, \qquad t \ge 0 \,, \qquad \ell \in [0, +\infty) \,. \tag{27}$$

A mathematical proof of both facts is still lacking, although several results in that direction have been obtained in [19]. Also, estimates for $T_{gel}$ are given in [23]. A more precise result is actually valid when $\mu = \nu = 1$: in that case, $T_{gel} = 1/M_2(0)$ is the blow-up time of the second moment $M_2$.

The main purpose of the numerical simulations presented in the next section is thus twofold: on the one hand, we aim at observing numerically the occurrence of gelation. On the other hand, we shall study the behavior of $f$ and its moments near the numerical gelation time and check whether it is consistent with the above conjectures.

**3.2. Test 3.1: $a(x, x') = (x\ x')^{\lambda/2}$, $\lambda \in (1, 2]$.** We restrict ourselves here to the model case (25) with $\mu = \nu = \lambda/2$; that is,

$$a(x, x') = (x\ x')^{\lambda/2} \,, \qquad (x, x') \in \mathbb{R}_+^2 \,,$$

with $\lambda \in (1, 2]$, and we take the following initial datum $f_0$:

$$g_0(x) = x\, f_0(x) = \exp(-x) \,, \qquad x \in \mathbb{R}_+ \,. \tag{28}$$

Since $\lambda > 1$, the gelation phenomenon does take place and $T_{gel} < +\infty$. Furthermore, for $\lambda = 2$, the Smoluchowski coagulation equation (1) has the explicit solution (22),

(23) for the initial datum (28), and the gelation time is $T_{gel} = 1$. We see in Figure 5 that the choice of the truncation (9) and the scheme (13) provides a good estimate of the exact gelation time.

Next, as recalled in the previous section, the moments $M_\ell(t)$ are expected to blow up as $t \to T_{gel}$ for $\ell \ge (1+\lambda)/2$ and to stay bounded if $\ell < (1+\lambda)/2$. For different values of $\lambda$, we compute numerical approximations of the solution to (1) with initial datum (28) for increasing values of the truncation parameter $R$. Recalling that $g^h$ is a numerical approximation of $g(t,x) = x\, f(t,x)$, we define the moment of order $\ell \ge 0$ of the numerical approximation by

$$\mathcal{M}_\ell^h(t^n) = \sum_{i=0}^{I^h} \Delta x_i \; x_i^{\ell-1} \; g_i^n \,,$$

and we plot the time evolution of the moments of order 1, $(1+\lambda)/2$, and 2 (see Figures 5, 6, and 7). It is clear that the gelation transition takes place in finite time and that there is a sudden growth of the moments of order $(1+\lambda)/2$ and 2 near the numerical gelation time. Since this growth increases with $R$, it seems to confirm the expected blow-up behavior. The fact that these moments decrease after the numerical gelation time is due to the finite length of the interval of computation. Let us also observe that the smaller $\lambda$ is, the larger the truncation parameter $R$ has to be taken for the numerical gelation time to "stabilize" near some value. This is, however, expected, since the gelation phenomenon becomes weaker as the parameter $\lambda$ comes closer to 1, and is thus more difficult to bring to the fore.

The last pictures in Figures 5, 6, and 7 are attempts to check numerically the validity of (26). Since the gelation time is not exactly known (except when $\lambda = 2$), it is not obvious how to obtain a reliable approximation of $f(T_{gel})$. In addition, the truncation greatly influences the large $x$-behavior after the numerical gelation time. The criterion we use here is to plot on the same picture the numerical solution shortly before and shortly after the gelation time and compute the slope of their common part. We then obtain rather good agreement with the expected behavior (26) for $\lambda$ sufficiently large ($\lambda \in \{3/2, 7/4, 2\}$), which seems to confirm the theory. Notice, however, that our results are slightly worse for $\lambda = 3/2$, and we believe that this is because we have not yet reached the convergence with respect to the truncation parameter $R$. Also, our results are in fair agreement with the numerical simulations performed in [31] and disagree with those reported in [26]. For smaller values of $\lambda \in (1,2]$, we still observe the occurrence of gelation, but it is more difficult to stabilize the numerical gelation time and to reproduce the correct behavior of $f$ at the gelation time. Possible reasons for this discrepancy are that the gelation time goes to infinity as $\lambda$ becomes closer to 1 and also that a much larger value of the truncation parameter $R$ is needed for the numerical gelation time to stabilize. Consequently, the computational cost and the numerical error are both increased, and a good approximation is thus harder to obtain.

**4. The nongelling case.** We next study the large time behavior of nongelling solutions to (1), that is, solutions for which gelation does not take place in finite time. We focus here on the multiplicative coagulation coefficient

$$a(x,x') = (x\,x')^{\lambda/2} \,, \qquad (x,x') \in \mathbb{R}_+^2 \,, \quad \lambda \in [0,1] \,, \tag{29}$$

and the additive coagulation coefficient

$$a(x,x') = x^\lambda + (x')^\lambda \,, \qquad (x,x') \in \mathbb{R}_+^2 \,, \quad \lambda \in [0,1] \,. \tag{30}$$

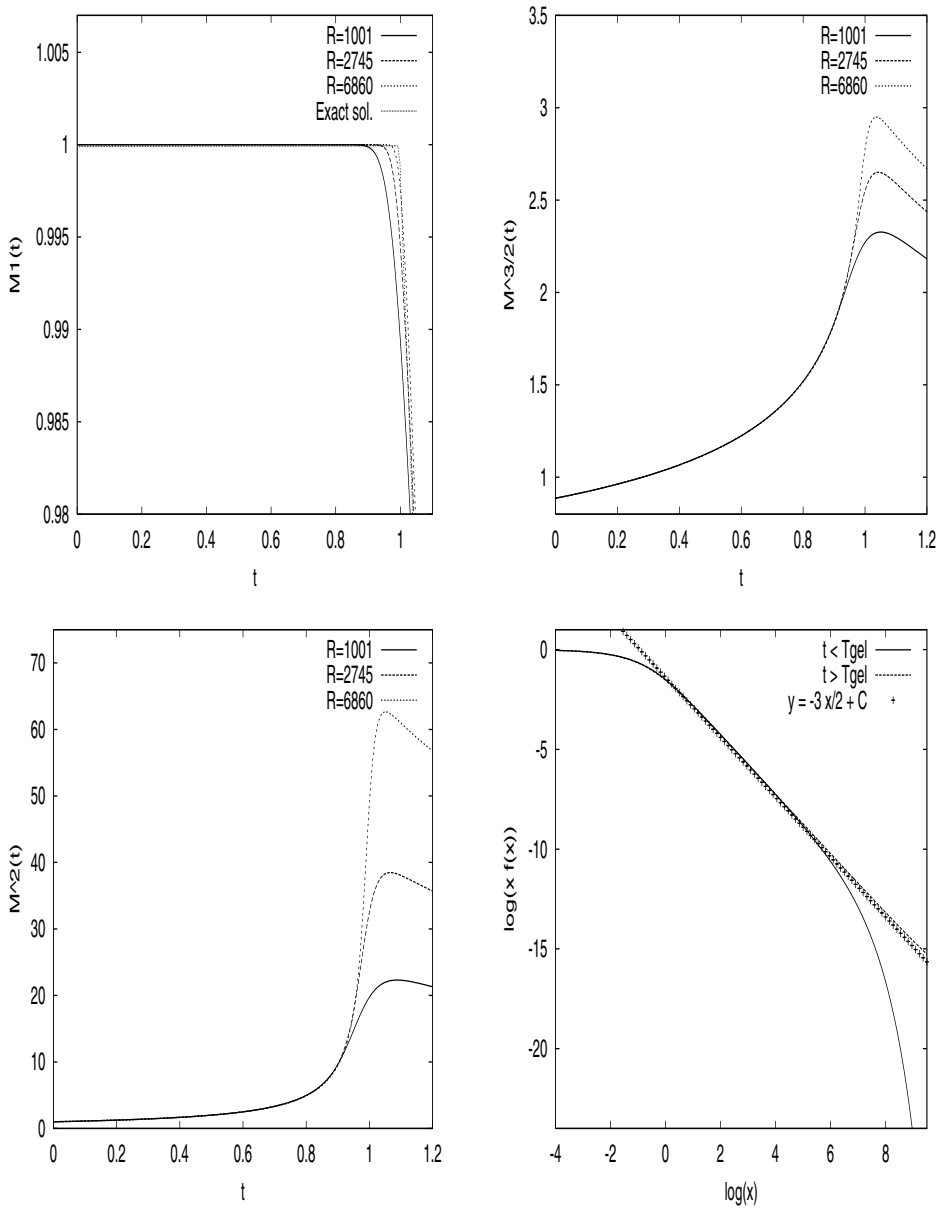


FIG. 5. *Test* 3.1 *with* $\lambda = 2$: *Time evolution of discrete moments of* $f(t)$, $\mathcal{M}^{h,1}(t)$, $\mathcal{M}^{h,3/2}(t)$, *and* $\mathcal{M}^{h,2}(t)$, *and the approximation of* $x\, f(t,x)$ *for* $t \simeq T_{gel}$.

In both cases, according to the discussion in section 3.1, we have $T_{gel} = +\infty$ since $\lambda \in [0,1]$ and thus

$$M_1(t) = M_1(0)\,, \qquad t \geq 0\,. \tag{31}$$

In this situation, a rather detailed description of the large time behavior of $f$ is conjectured by physicists and is known as the *dynamical scaling hypothesis* (see, e.g., [11] and the references therein). More precisely, the volume distribution function $f$ is

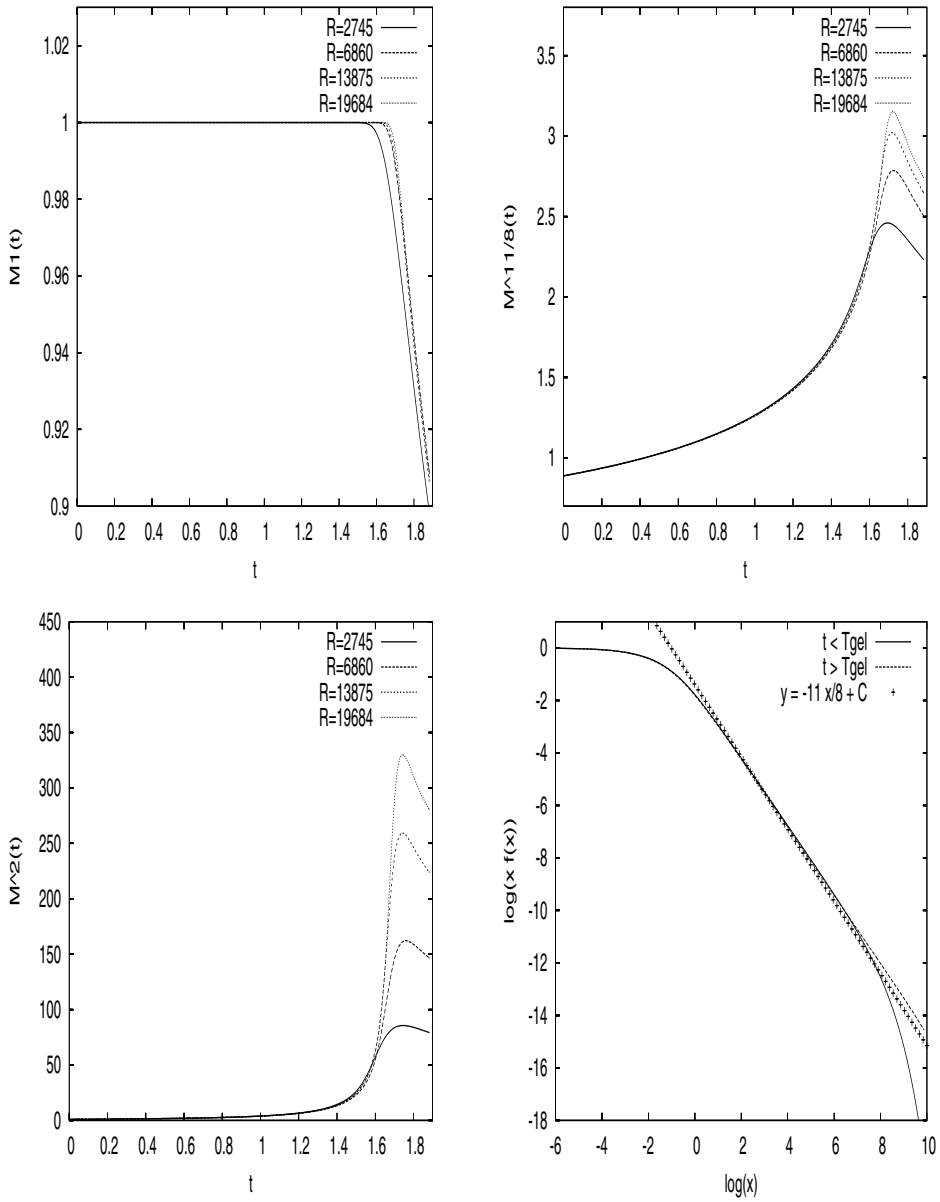


FIG. 6. *Test* 3.1 *with* $\lambda = 7/4$: *Time evolution of discrete moments of* $f(t)$, $\mathcal{M}^{h,1}(t)$, $\mathcal{M}^{h,11/8}(t)$, *and* $\mathcal{M}^{h,2}(t)$, *and the approximation of* $x\, f(t,x)$ *for* $t \simeq T_{gel}$.

expected to behave in a self-similar way in the long time,

$$f(t,x) \underset{t\to+\infty}{\sim} f_S(t,x) := \frac{1}{s(t)^2}\, \varphi\left(\frac{x}{s(t)}\right) , \tag{32}$$

where the mean volume $s(t)$ and the profile $\varphi$ are to be determined and depend on $a$ but not on the "details" of the initial data. Furthermore, $f_S$ is actually expected to

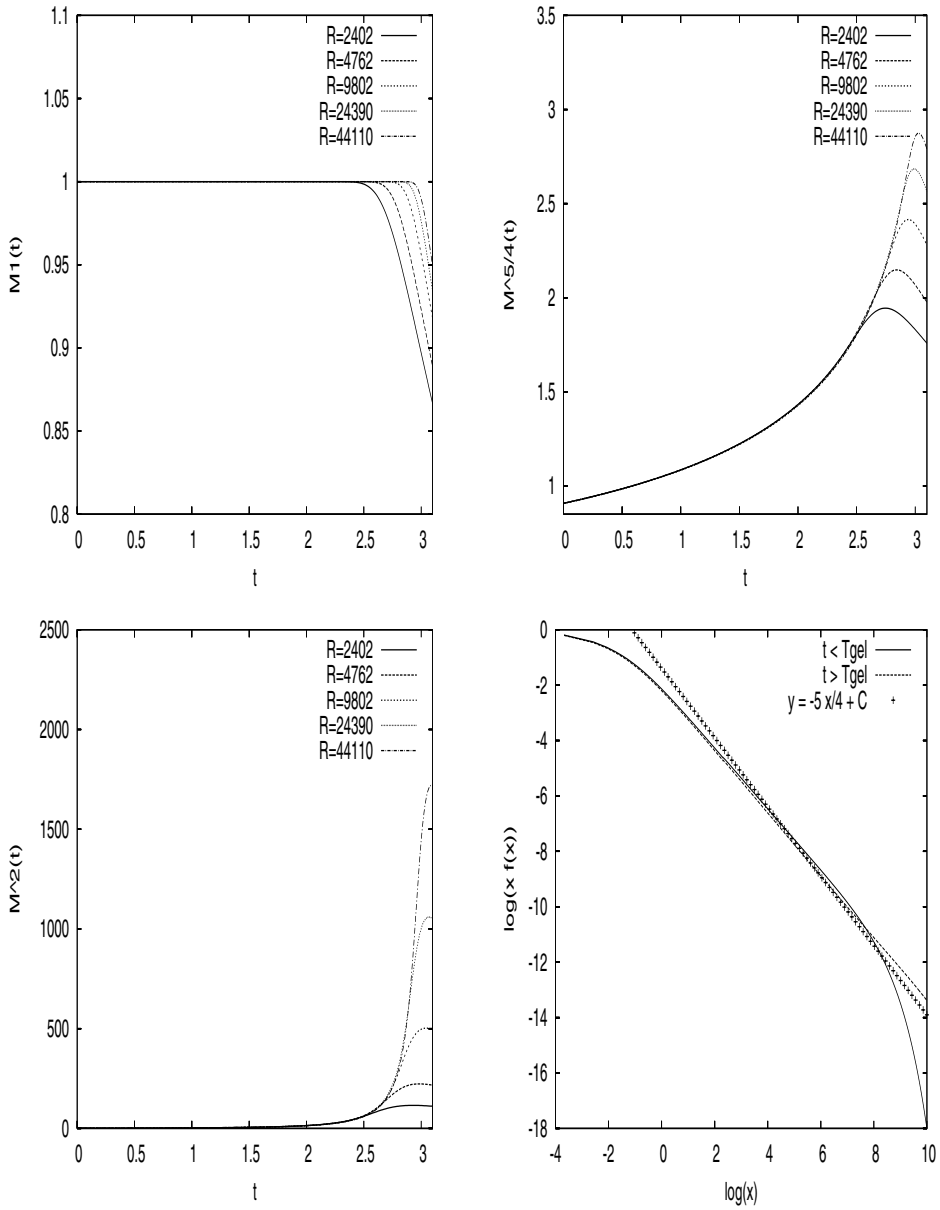


FIG. 7. *Test* 3.1 *with* $\lambda = 3/2$: *Time evolution of discrete moments of* $f(t)$, $\mathcal{M}^{h,1}(t)$, $\mathcal{M}^{h,5/4}(t)$, *and* $\mathcal{M}^{h,2}(t)$, *and the approximation of* $x\, f(t,x)$ *for* $t \simeq T_{gel}$.

be a self-similar solution to (1), from which we deduce that, if $\lambda < 1$,

$$\frac{ds}{dt}(t) = w\ s(t)^{\lambda} \tag{33}$$

and

$$w\ x^2\ \varphi(x) - J(\varphi)(x) = 0\,, \qquad x \in (0, +\infty)\,, \tag{34}$$

the parameter $w > 0$ being a separation constant for the $x$ and $t$ dependence [11] (recall that $J$ is given by (6)). We exclude here the case $\lambda = 1$, which is more complicated, and refer to [11] for a complete discussion.

Unfortunately, nothing much is known from the rigorous point of view about the validity of (32). Even the existence of a solution to (34) is still an open problem except when $a(x, x') = 1$ or $a(x, x') = x + x'$. In these two cases, explicit formulae for $\varphi$ are known [11] and convergence results have been established in [1, 5, 9, 25, 29]. In the other cases, numerical simulations have been performed to check the validity of (32) [21, 26, 30, 31]. Also, numerical studies of the behavior of $\varphi$ for large and small values of $x$ have been done in [7, 36] for comparison with the formal predictions from [11]. Numerical simulations reported in the above-mentioned papers are performed directly on (1) on a sufficiently large time, and there needs to be a compromise between computational cost and numerical precision. Also, the convergence toward self-similarity could possibly be very slow, and the accumulation of numerical errors on a large time interval could spoil the result.

We thus propose to proceed in an alternative way based on the following classical observation. An equivalent formulation of (32) is

$$s(t)^2 \ f(t, x\, s(t)) \underset{t \to +\infty}{\sim} \varphi(x)\,,$$

from which we realize that the convergence (32) of $f$ toward $f_S$ translates to the convergence of $(t, x) \longmapsto s(t)^2 \ f(t, x\, s(t))$ to a stationary state. Since we believe that such a convergence is more stable from a numerical viewpoint, we shall thus first perform a change of variables in (1).

REMARK 4.1. *Assuming further that the initial total volume $M_1(0)$ is the only parameter which rules over the large time behavior, scaling arguments allow us to set $w = 1$, using again the fact that $\lambda < 1$. The situation is indeed different when $\lambda = 1$: for instance, for the additive coefficient* (30) *with $\lambda = 1$, it follows from* [9, 11] *that the large time behavior is determined by $M_1(0)$ and $M_2(0)$ (if the latter is finite; the situation is more complicated otherwise* [5]*).*

**4.1. Self-similar variables.** From now on, we assume that $a$ is given by either (29) or (30) with $\lambda \in [0, 1)$. Let $f$ be a solution to the coagulation equation (1). Owing to Remark 4.1, we set

$$s(t) = (1 + (1 - \lambda)\, t)^{1/(1-\lambda)}\,, \qquad t \ge 0\,, \tag{35}$$

and

$$f(t, x) = \frac{1}{s(t)^2} \ \psi\left(\ln s(t), \frac{x}{s(t)}\right)\,, \qquad (t, x) \in \mathbb{R}_+^2\,. \tag{36}$$

Then, $\psi$ solves (in a weak sense)

$$x \ \partial_t \psi = \partial_x \left(x^2 \ \psi - J(\psi)\right)\,, \qquad (t, x) \in \mathbb{R}_+^2\,, \tag{37}$$

with $\psi(0) = f(0) = f_0$. Observe that the profile $\varphi$ in (32) is a stationary solution to (37) by (34) so that the conjecture (32) becomes

$$\psi(t) \longrightarrow \varphi \quad \text{as} \quad t \to +\infty\,, \tag{38}$$

where $\varphi$ is a stationary solution to (37) depending only on the initial volume $M_1(0)$.

The discretization of the Smoluchowski equation in self-similar variables (37) requires more attention since there is an additional term $\partial_x\left(x^2\,\psi\right)$, which can be very costly to compute by a time explicit scheme. Indeed, recalling that we compute an approximation of $x\psi(t,x)$, it leads to a CFL condition of the form

$$C\,x_{I^h+1/2}\,\frac{\Delta t}{h} \le 1\,,$$

which becomes more restrictive as $R$ increases. To avoid such a condition, we use a semi-implicit scheme (that is, explicit for the nonlinear part and implicit for the linear one), which reads

$$g_i^{n+1} = g_i^n + \frac{\Delta t}{\Delta x_i}\left(x_{i+1/2}\;g_{i+1}^{n+1} - x_{i-1/2}\;g_i^{n+1}\right) - \frac{\Delta t}{\Delta x_i}\left(J_{i+1/2}^{h,n} - J_{i-1/2}^{h,n}\right) \tag{39}$$

for $0 \le i \le I^h$ with the boundary condition

$$g_{I^h+1}^{n+1} = 0\,. \tag{40}$$

In (39), $g_i^n$ denotes the approximation of $x\,\psi(t,x)$ for $(t,x) \in [t^n, t^{n+1}) \times \Lambda_i^h$, and $J_{i+1/2}^{h,n}$ is still given by (14). Let us point out that the solution of this algebraic system can be found without solving any linear system thanks to (40).

On the other hand, since we are working in self-similar variables, the transfer of mass to the right due to $J(\psi)$ in (37) is balanced by the term $x^2\psi$ so that there is no longer a drift of the distribution function toward larger and larger volumes. Thus, solutions to (37) with rapidly decaying initial data are expected to keep the same decay through time evolution, and the numerical results are less sensitive to the choice of $R$ (as soon as it is sufficiently large).

**4.2. Test 4.1: $a(x,x') = (x^\lambda + (x')^\lambda)$, $\lambda \in (0,1)$.** We first check the validity of (38) and perform numerical simulations for different initial data having the same initial total volume $M_1(0)$. We then observe that the numerical solutions converge to a stationary state, which remains approximatively the same. We next consider the following initial data:

$$f_0(x) = \exp(-x), \quad x \ge 0\,.$$

We then study the time evolution of different moments of $f$ (of order $\lambda$, 1, 2) and the behavior of the asymptotic profile $x\;f(+\infty,x)$ of $x\;f(t,x)$ for $x \sim 0$ as well. Concerning the latter, it is worth mentioning that it is conjectured in [11] that the profile $\varphi$ in (38) has the following behavior for small $x$:

$$\varphi(x) \underset{x\to 0}{\sim} B\;x^{-\tau}\,, \tag{41}$$

where the exponent $\tau$ is determined implicitly by $\tau = 2 - M_\lambda(\varphi)$, $M_\lambda(\varphi)$ being the moment of order $\lambda$ of $\varphi$. Numerical computations of the exponent $\tau$ have been performed in [7, 26, 30, 31] for the more general coagulation coefficient $a(x,x') = (x^{1/D} + x'1/D)^d$ for some values of $d > 0$ and $D > 0$. The most complete study was performed in [7], where a method to compute $\tau$ without solving (1) was developed.

From a numerical point of view, some care is needed to compute the small $x$-behavior of the stationary state, taking into account that it also depends on its values for large $x$ through the second integral in $J(\psi)$. Therefore, it is important to consider

a suitable mesh in order to obtain an accurate numerical solution when $x$ is small (i.e., of order $10^{-6}$) but also for large $x$. We construct the following mesh: we fix $\Delta y > 0$ and put $y_i = m + i\,\Delta y$ and

$$x_i = \begin{cases} \exp(y_i) & \text{for } y_i \le 0\,, \\ y_i^2 & \text{for } 1 \le y_i \le R^{1/2}\,, \end{cases}$$

for $i \in \{0, \ldots, n_x - 1\}$, where $m < 0 < R$ are chosen with respect to the initial data and $\lambda$. With this choice, $(\log(x_i))_i$ is a uniform mesh of $[m, 0]$. Moreover, the choice of a mesh of order $O(y_i^2)$ for larger $x$ allows us to use a sufficiently large truncation when the support of $f$ is increasing.

In Figures 8, 9, and 10, we report the evolution of the $\lambda$th and second moments of $f$ and the behavior of the asymptotic profile $x\ f(+\infty, x)$ for $x \sim 0$ for different values of $\lambda$. As expected, the total volume $M_1(t)$ remains constant throughout time evolution and the second moment stabilizes to some value. As for the small $x$-behavior of the asymptotic profile, our numerical results are in fair agreement with those previously obtained by different authors with other methods [7, 31]. In Table 1, we report the values of $\tau$ obtained numerically in [7, 31] in the first line and the values of $\tau$ resulting from our numerical simulations in the second line. In the last line we report the value of $2 - M_\lambda(\varphi)$ obtained from our numerical simulations to check the validity of the conjecture $\tau = 2 - M_\lambda(\varphi)$. Our numerical results thus support the validity of the conjecture (41).

**4.3. Test 4.2: $a(x, x') = (x\ x')^{\lambda/2}$, $\lambda \in (0, 1)$.** Again, we first check the validity of (38) and perform numerical simulations for different initial data having the same initial total volume $M_1(0)$. We choose initial data of the form

$$f_0(x) = \frac{x^n}{(n+1)!}\,\exp(-x), \quad n \in \{0, 1, 2, \ldots\}.$$

We then observe that the numerical solutions converge to a stationary state, which remains approximatively the same. We next consider the initial data

$$f_0(x) = \exp(-x), \quad x \ge 0\,,$$

and focus on the time evolution of the first and second moment of $f$ and on the behavior of the asymptotic profile $x\ f(+\infty, x)$ for $x \sim 0$. We first recall that it is conjectured in [11] that the profile $\varphi$ in (38) has the following behavior for small $x$:

$$\varphi(x) \underset{x \to 0}{\sim} B\ x^{-(1+\lambda)}\,. \tag{42}$$

Numerical simulations have already been performed in that case in [26, 31]. On the one hand, the outcome of [26] disagrees with the conjectured behavior (42) for $\varphi$, but, as already pointed out in [31], it seems that the computations in [26] have not been done on a sufficiently long time interval. On the other hand, there is a fair agreement between the theoretical predictions (42) and the numerical simulations of [31], although an oscillatory behavior is reported in that paper. Our numerical simulations are in good agreement with the theoretical predictions (42).

A damped oscillatory behavior around the prediction (42) is also observed in our simulations (although with smaller amplitudes), but in a region which is close to but separated from $x = 0$, of the form $[10^{-p}, 1]$, where $p \sim 15$ if $\lambda = 2/3$, $p \sim 25$ if $\lambda = 1/2$ and $p \sim 40$ if $\lambda = 1/3$. In the region $(0, 10^{-p})$, our simulations are in good

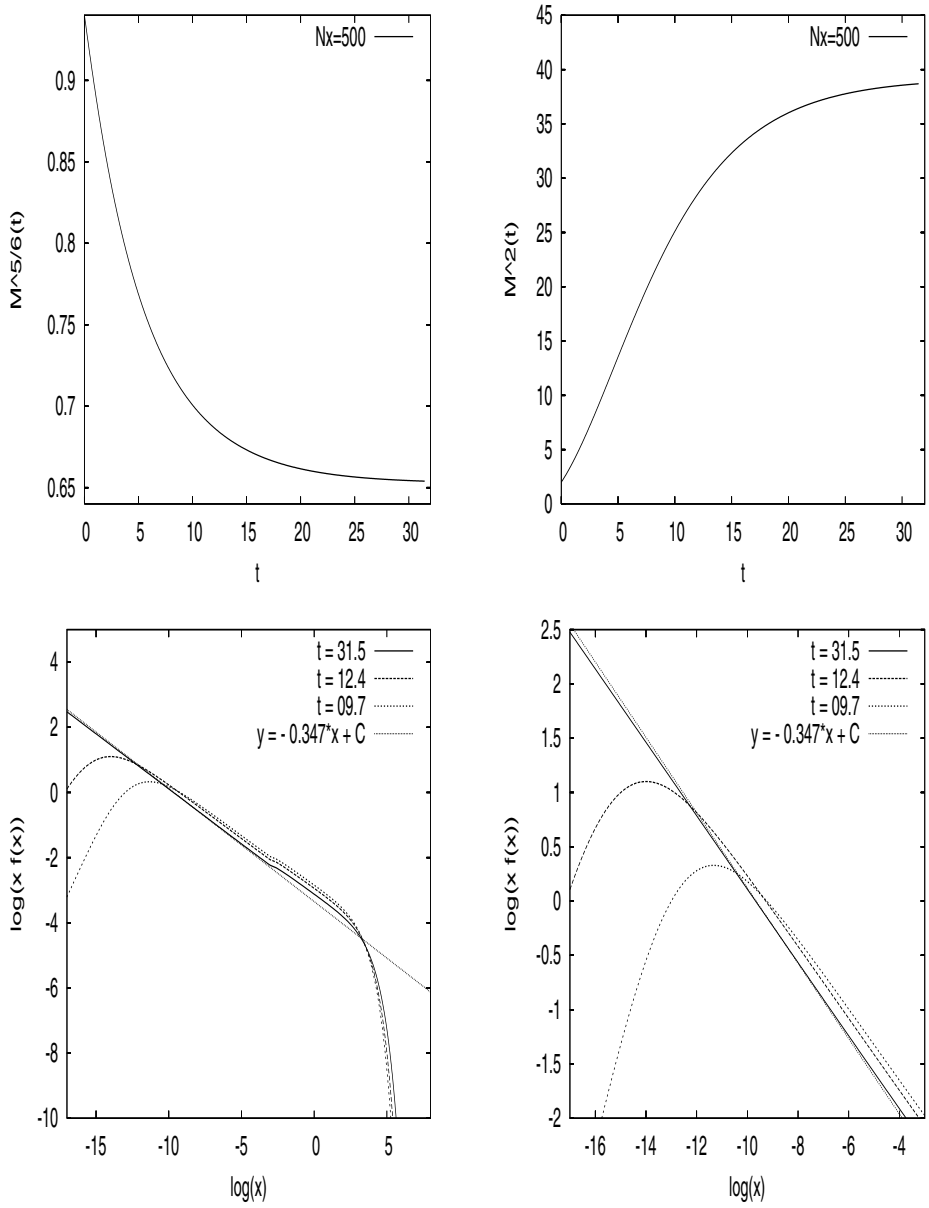


FIG. 8. *Test* 4.1 *with* $\lambda = 5/6$: *Evolution of the* $5/6$*th and second moments of* $f$ *and the stationary distribution* $x\ f(x)$ *in log scale.*

agreement with the conjecture (42) as seen in the right-bottom pictures of Figures 11, 12, and 13. We thus believe that the simulations reported in [31] were not done on a sufficiently long time interval since the lowest volume reached is of order $t^{-1/1-\lambda}$. Attaining volumes lower that $10^{-p}$ would require that $t > 10^{p(1-\lambda)} \sim 10^5$ if $\lambda = 2/3$, $t > 10^{12}$ if $\lambda = 1/2$, and $t > 10^{27}$ if $\lambda = 1/3$. By the way, this is a nice feature of working in self-similar variables to perform computations on a time interval including very small volumes in a reasonable amount of time.

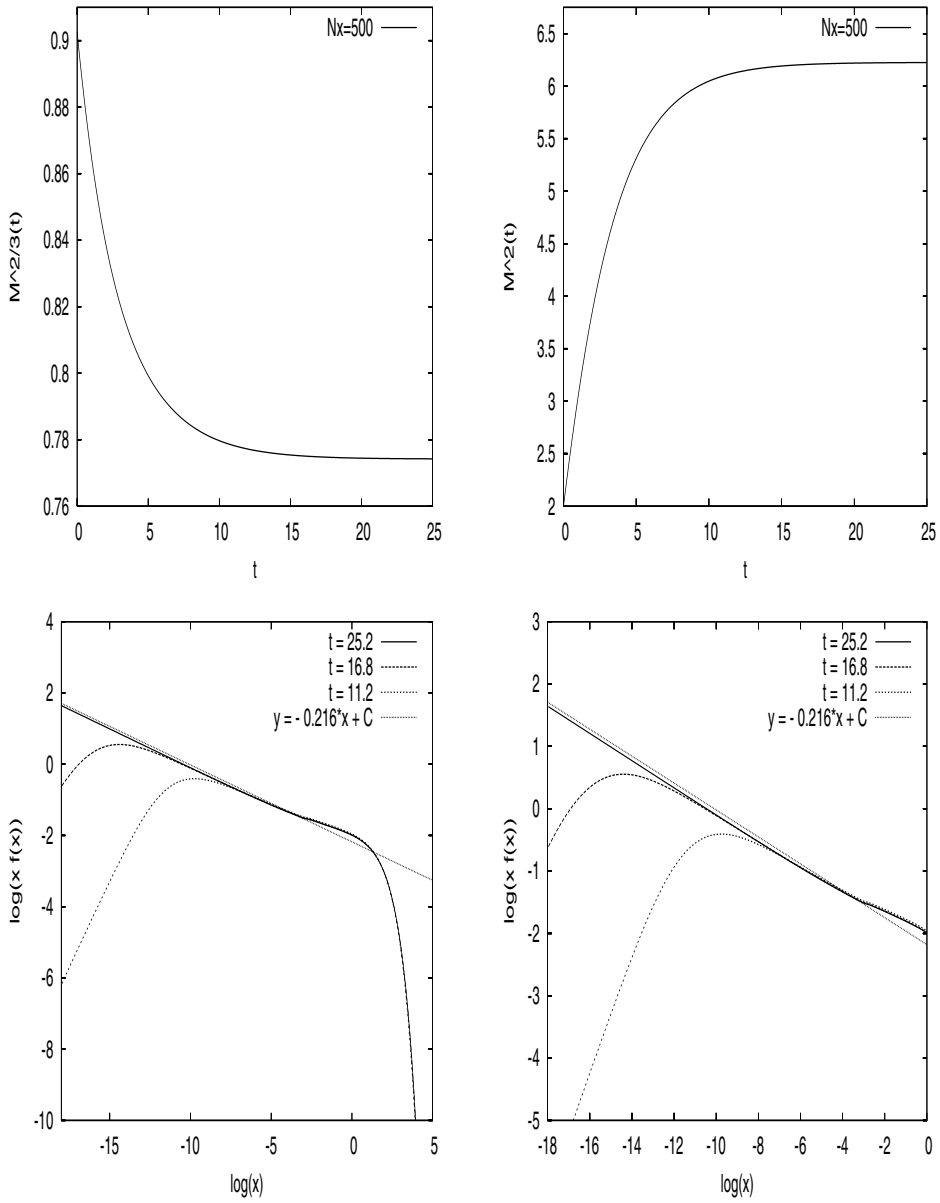


FIG. 9. *Test* 4.1 *with* $\lambda = 2/3$: *Evolution of the* $2/3$*rd and second moments of* $f$ *and the stationary distribution* $x\ f(x)$ *in log scale.*

Also, performing the numerical simulations on (37) written in self-similar variables allows us to use a smaller truncation parameter $R$ and a smaller final time and thus reduces the numerical error.

**5. Conclusion.** We have proposed and implemented a numerical scheme for the Smoluchowski coagulation equation (1) which relies on the conservative formulation (5) of (1). Comparison with explicit solutions shows the convergence of the scheme which turns out to be second order accurate. We have next performed several numer-

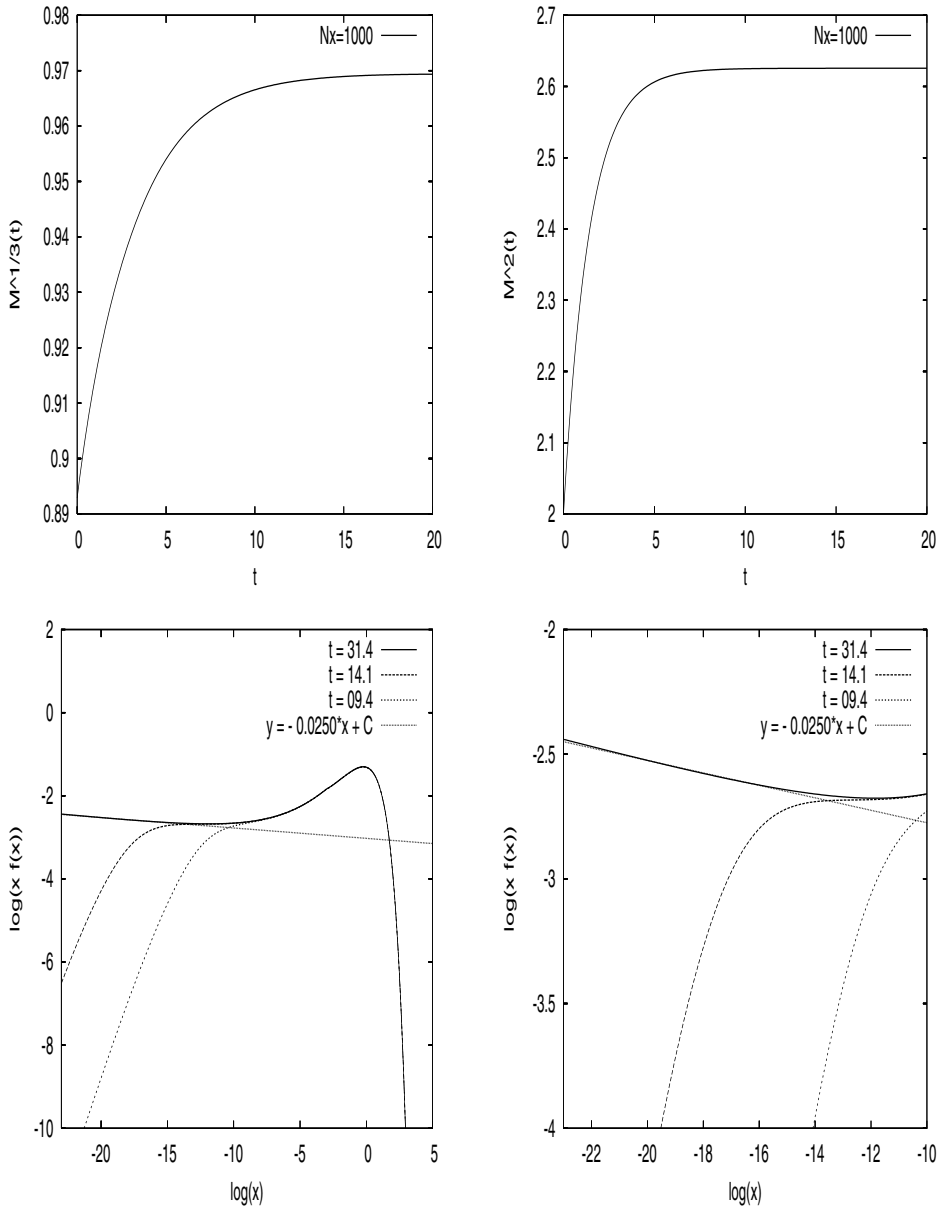


FIG. 10. *Test* 4.1 *with* $\lambda = 1/3$: *Evolution of the* 1/3*rd and second moments of* $f$ *and the stationary distribution* $x\ f(x)$ *in log scale.*

TABLE 1

*Values of the exponent* $\tau$ *giving the behavior of* $x\ f(+\infty, x)$ *for* $x$ *close to zero when* $a(x, x') = x^\lambda + (x')^\lambda$.

| $\lambda$ | 1.0 | 5/6 | 2/3 | 1/2 | 1/3 |
|---|---|---|---|---|---|
| $\tau$ [7, 31] | 1.50 | 1.347 | 1.216 | 1.109 | 1.033 |
| $\tau$ | 1.50 | 1.347 | 1.216 | 1.090 | 1.025 |
| 2-$M_\lambda(f)$ | 1.50 | 1.347 | 1.220 | 1.100 | 1.031 |

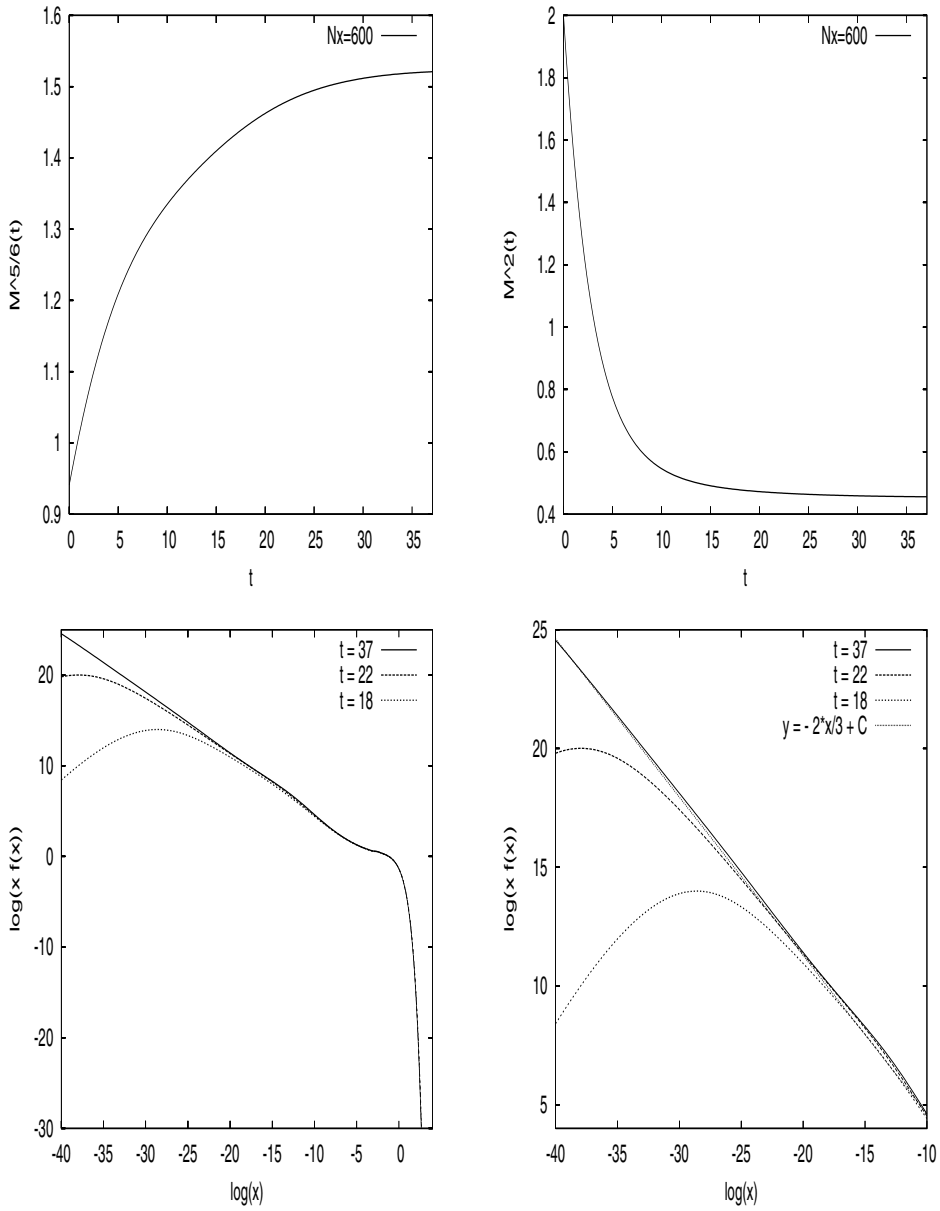


FIG. 11. *Test* 4.2 *with* $\lambda = 2/3$: *Evolution of* $(\lambda+1)/2nd$ $(5/6)$ *and second moments of* $f$ *and the distribution function* $x\ f(x)$ *in log scale for large time.*

ical simulations to check the known or conjectured behavior of the solution near the gelation time or as time increases to infinity. In the latter case, we also have checked the validity of the dynamical scaling hypothesis. In both cases, our numerical simulations are in good agreement with physical conjectures. To summarize, the numerical method developed in this paper presents the following advantages:

- The equation in conservative form is well suited for the discretization using the finite volume approach.

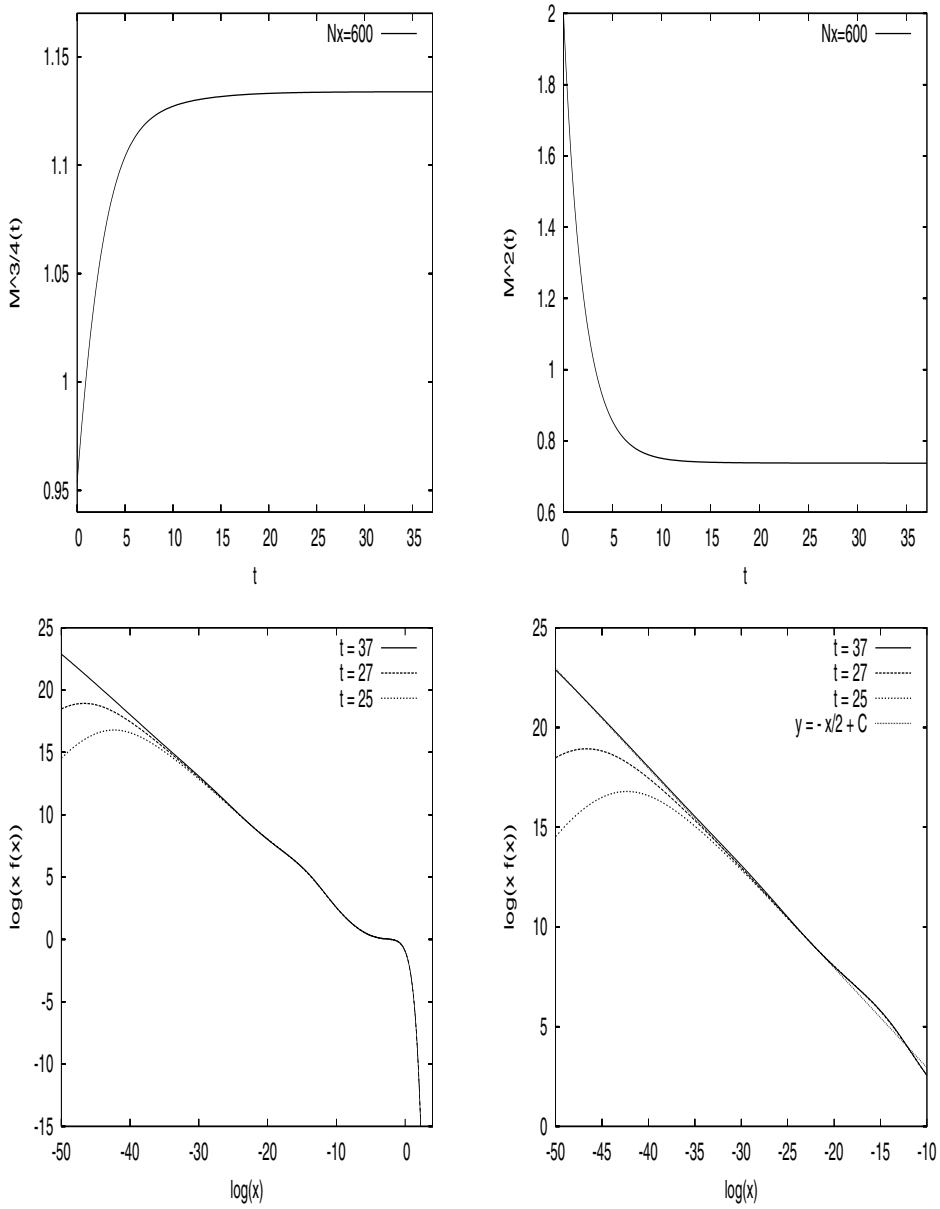


FIG. 12. *Test* 4.2 *with* $\lambda = 1/2$: *Evolution of* $(\lambda+1)/2$*nd and second moments of* $f$ *and the distribution function* $x\ f(x)$ *in log scale for large time.*

- The rescaling of the equation allows us to work on a smaller domain in volume, and the time scale is highly reduced.
- The finite volume method gives accurate results and is very robust for nonuniform meshes. Furthermore, the mesh can be adapted to the shape of the solution in order to accurately describe its singular behavior for small values of the volume.

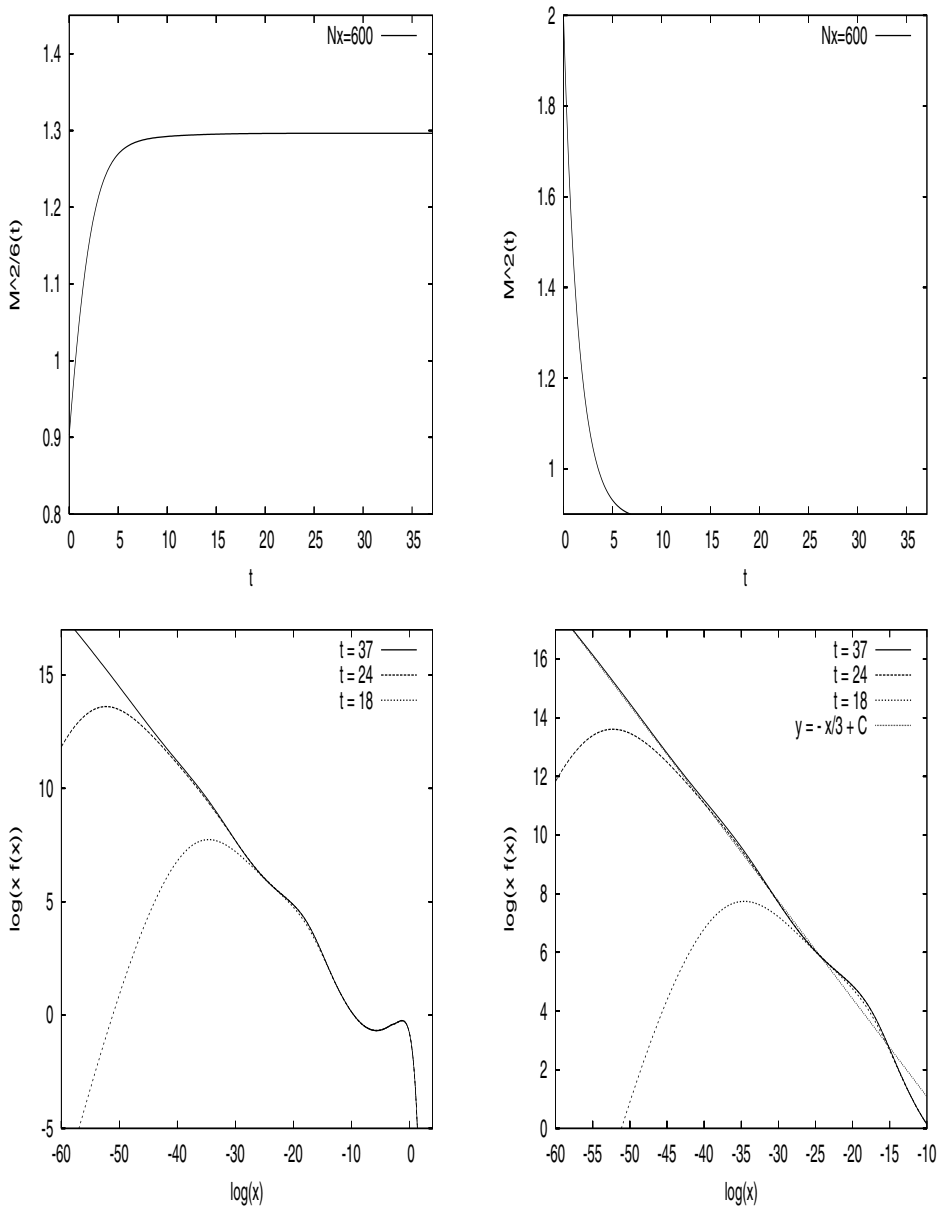


FIG. 13. *Test* 4.2 *with* $\lambda = 1/3$: *Evolution of* $(\lambda+1)/2nd$ $(2/3)$ *and second moments of* $f$ *and the distribution function* $x\ f(x)$ *in log scale for large time.*

**Acknowledgments.** We thank Ch. Giraud and E. Tanré for interesting discussions.

REFERENCES

[1] D. J. ALDOUS, *Deterministic and stochastic models for coalescence (aggregation, coagulation): A review of the mean-field theory for probabilists*, Bernoulli, 5 (1999), pp. 3–48.

[2] H. Babovsky, *On a Monte Carlo scheme for Smoluchowski's coagulation equation*, Monte Carlo Methods Appl., 5 (1999), pp. 1–18.
[3] T. A. Bak and O. Heilmann, *A finite version of Smoluchowski's coagulation equation*, J. Phys. A, 24 (1991), pp. 4889–4893.
[4] J. M. Ball and J. Carr, *The discrete coagulation-fragmentation equations: Existence, uniqueness, and density conservation*, J. Statist. Phys., 61 (1990), pp. 203–234.
[5] J. Bertoin, *Eternal solutions to Smoluchowski's coagulation equation with additive kernel and their probabilistic interpretation*, Ann. Appl. Probab., 12 (2002), pp. 547–564.
[6] F. P. da Costa, *A finite-dimensional dynamical model for gelation in coagulation processes*, J. Nonlinear Sci., 8 (1998), pp. 619–653.
[7] S. Cueille and C. Sire, *Nontrivial polydispersity exponents in aggregation models*, Phys. Rev. E (3), 55 (1997), pp. 5465–5478.
[8] M. Deaconu, N. Fournier, and E. Tanré, *Study of a stochastic particle system associated with the Smoluchowski coagulation equation*, Methodol. Comput. Appl. Probab., 5 (2003), pp. 131–158.
[9] M. Deaconu and E. Tanré, *Smoluchowski's coagulation equation: Probabilistic interpretation of solutions for constant, additive and multiplicative kernels*, Ann. Scuola Norm. Sup. Pisa Cl. Sci. (4), 29 (2000), pp. 549–579.
[10] P. G. J. van Dongen and M. H. Ernst, *Cluster size distribution in irreversible aggregation at large times*, J. Phys. A, 18 (1985), pp. 2779–2793.
[11] P. G. J. van Dongen and M. H. Ernst, *Scaling solutions of Smoluchowski's coagulation equation*, J. Statist. Phys., 50 (1988), pp. 295–329.
[12] R. L. Drake, *A general mathematical survey of the coagulation equation*, in Topics in Current Aerosol Research (Part 2), International Reviews in Aerosol Physics and Chemistry, Pergamon Press, Oxford, UK, 1972, pp. 203–376.
[13] P. B. Dubovskiĭ and I. W. Stewart, *Existence, uniqueness and mass conservation for the coagulation-fragmentation equation*, Math. Methods Appl. Sci., 19 (1996), pp. 571–591.
[14] A. Eibeck and W. Wagner, *An efficient stochastic algorithm for studying coagulation dynamics and gelation phenomena*, SIAM J. Sci. Comput., 22 (2000), pp. 802–821.
[15] A. Eibeck and W. Wagner, *Stochastic particle approximations for Smoluchowski's coagulation equation*, Ann. Appl. Probab., 11 (2001), pp. 1137–1165.
[16] L. D. Erasmus, D. Eyre, and R. C. Everson, *Numerical treatment of the population balance equation using a Spline-Galerkin method*, Computers Chem. Engrg., 8 (1994), pp. 775–783.
[17] M. H. Ernst, R. M. Ziff, and E. M. Hendriks, *Coagulation processes with a phase transition*, J. Colloid Interface Sci., 97 (1984), pp. 266–277.
[18] M. Escobedo, Ph. Laurençot, S. Mischler, and B. Perthame, *Gelation and mass conservation in coagulation-fragmentation models*, J. Differential Equations, 195 (2003), pp. 143–174.
[19] M. Escobedo, S. Mischler, and B. Perthame, *Gelation in coagulation and fragmentation models*, Comm. Math. Phys., 231 (2002), pp. 157–188.
[20] F. Filbet and Ph. Laurençot, *Mass-conserving solutions and non-conservative approximation to the Smoluchowski coagulation equation*, Arch. Math. (Basel), to appear.
[21] S. K. Friedlander and C .S. Wang, *The self-preserving particle size distribution for coagulation by brownian motion*, J. Colloid Interface Sci., 22 (1966), pp. 126–132.
[22] F. Guiaş, *A Monte Carlo approach to the Smoluchowski equations*, Monte Carlo Methods Appl., 3 (1997), pp. 313–326.
[23] E. M. Hendriks, M. H. Ernst, and R. M. Ziff, *Coagulation equations with gelation*, J. Statist. Phys., 31 (1983), pp. 519–563.
[24] I. Jeon, *Existence of gelling solutions for coagulation-fragmentation equations*, Comm. Math. Phys., 194 (1998), pp. 541–567.
[25] M. Kreer and O. Penrose, *Proof of dynamical scaling in Smoluchowski's coagulation equation with constant kernel*, J. Statist. Phys., 75 (1994), pp. 389–407.
[26] D. S. Krivitsky, *Numerical solution of the Smoluchowski kinetic equation and asymptotics of the distribution function*, J. Phys. A, 28 (1995), pp. 2025–2039.
[27] Ph. Laurençot, *On a class of continuous coagulation-fragmentation equations*, J. Differential Equations, 167 (2000), pp. 145–174.
[28] Ph. Laurençot and S. Mischler, *From the discrete to the continuous coagulation-fragmentation equations*, Proc. Roy. Soc. Edinburgh Sect. A, 132 (2002), pp. 1219–1248.
[29] Ph. Laurençot and S. Mischler, in preparation.
[30] M. H. Lee, *On the validity of the coagulation equation and the nature of runaway growth*, Icarus, 143 (2000), pp. 74–86.
[31] M. H. Lee, *A survey of numerical solutions to the coagulation equation*, J. Phys. A, 34 (2001),

pp. 10219–10241.
[32] F. Leyvraz, *Existence and properties of post-gel solutions for the kinetic equations of coagulation*, J. Phys. A, 16 (1983), pp. 2861–2873.
[33] F. Leyvraz and H. R. Tschudi, *Singularities in the kinetics of coagulation processes*, J. Phys. A, 14 (1981), pp. 3389–3405.
[34] F. Leyvraz and H. R. Tschudi, *Critical kinetics near gelation*, J. Phys. A, 15 (1982), pp. 1951–1964.
[35] J. Makino, T. Fukushige, Y. Funato, and E. Kokubo, *On the mass distribution of planetesimals in the early runaway stage*, New Astronomy, 3 (1998), pp. 411–417.
[36] A. Meesters and M. H. Ernst, *Numerical evaluation of self-preserving spectra in Smoluchowski's coagulation theory*, J. Colloid Interface Sci., 119 (1987), pp. 576–587.
[37] K. K. Sabelfeld and A. A. Kolodko, *Monte Carlo simulation of the coagulation processes governed by Smoluchowski equation with random coefficients*, Monte Carlo Methods Appl., 3 (1997), pp. 275–311.
[38] M. Smoluchowski, *Drei Vorträge über Diffusion, Brownsche Molekularbewegung und Koagulation von Kolloidteilchen*, Physik. Zeitschr., 17 (1916), pp. 557–599.
[39] I. W. Stewart, *A global existence theorem for the general coagulation-fragmentation equation with unbounded kernels*, Math. Methods Appl. Sci., 11 (1989), pp. 627–648.
[40] H. Tanaka, S. Inaba, and K. Nakaza, *Steady-state size distribution for the self-similar collision cascade*, Icarus, 123 (1996), pp. 450–455.
[41] W. H. White, *A global existence theorem for Smoluchowski's coagulation equations*, Proc. Amer. Math. Soc., 80 (1980), pp. 273–276.